

1 **Title:** Agnostic fungi: plant functional types and tissue stoichiometry explain nutrient transfer in
2 common arbuscular mycorrhizal networks of temperate grasslands

3
4 **Authors:** Hilary Rose Dawson^{1,2*}, Katherine L. Shek^{1,2,3}, Toby M. Maxwell^{1,4}, Paul B. Reed^{1,2,5},
5 Barbara Bomfim^{1,6}, Scott D. Bridgham^{1,2}, Brendan J. M. Bohannan^{1,2}, Lucas C.R. Silva^{1,2,7*}

6
7 **Affiliations:**

8 1. Institute of Ecology and Evolution, University of Oregon, Eugene, OR 97403 USA

9 2. Department of Biology, University of Oregon, Eugene, OR 97403 USA

10 3. Department of Natural Resources and the Environment, University of New Hampshire,
11 Durham NH 03824

12 4. Department of Biological Sciences, Boise State University, Boise, Idaho, 83725 USA

13 5. Institute for Applied Ecology, Corvallis, OR 97333 USA

14 6. Climate and Ecosystem Sciences Division, Lawrence Berkeley National Laboratory, Berkeley,
15 CA 94720 USA

16 7. Environmental Studies Program, University of Oregon, Eugene, OR 97403 USA

17
18 **Corresponding authors:** H.R.D. hilaryd@uoregon.edu L.C.R.S. lsilva7@uoregon.edu

19
20 **ORCID:**

21 H.R.D.: 0000-0003-4613-762X

22 K.L.S.: 0000-0001-5629-5782

23 T.M.M.: 0000-0001-5171-0705

24 P.B.R.: 0000-0001-7143-7515

25 B.B.: 0000-0001-9510-2496

26 S.D.B.: 0000-0003-0614-2678

27 B.J.M.B.: 0000-0003-2907-1016

28 L.C.R.S.: 0000-0002-4838-327X

29

30

31 **Summary:**

32 Plants and mycorrhizal fungi form close mutualistic relationships that affect how resources flow
33 between organisms and within ecosystems. Common mycorrhizal networks (CMNs) could
34 facilitate preferential transfer of carbon and limiting nutrients but this preference remains
35 difficult to predict. Do common mycorrhizal networks favor fungal growth at the expense of
36 plant resource demands (a fungi-centric view), or are they passive channels through which plants
37 regulate resource fluxes (a plant-centric view)? We used stable isotope tracers (^{13}C and ^{15}N),
38 plant traits, and fungal DNA, to quantify above- and belowground allocation and transfer of
39 carbon and nitrogen between 18 plant species in restored prairie and introduced pasture systems
40 in the Pacific Northwest, USA. We found that related plant species and connectivity with fungal
41 communities did not predict resource flow. Instead, plant functional type and tissue
42 stoichiometry were the most important predictors of interspecific resource transfer. Labeled
43 "donor" plants assimilated isotopic tracers at similar rates; however, nitrogen was preferentially
44 transferred to annual and forb "receiver" plants compared to perennial and grass receiver plants.
45 This corresponded tissue stoichiometry differences. Our findings point to a simple mechanistic
46 answer for long-standing questions regarding mutualism and transfer of resources between plants
47 via mycorrhizal networks.

48

49 **Keywords:** arbuscular mycorrhizal fungi, carbon, common mycorrhizal networks, ecological
50 stoichiometry, grasslands, nitrogen, plant functional type

51 **Introduction:**

52 Plant-mycorrhizal associations are thought to have emerged as rudimentary root systems
53 over 400 million years ago, facilitating the expansion of terrestrial life that followed (Kenrick &
54 Strullu-Derrien, 2014). The transformative power of early fungal symbioses is still evident today
55 in all major plant lineages, from bryophytes to angiosperms (van der Heijden *et al.*, 2015). Over
56 85% of all contemporary flowering plant species form symbioses with fungi, with arbuscular
57 mycorrhizal (AM) associations being the most common (Brundrett, 2009). Today, the
58 relationships between plants and AM fungi dominates both managed and unmanaged landscapes
59 and are estimated to be responsible for up to 80% of global primary productivity (van der
60 Heijden *et al.*, 2015). Fungi are gregarious and form symbioses with more than one individual
61 plant (Selosse *et al.*, 2006). By extension, it has been widely hypothesized that the multi-plant-
62 fungal relationships form “common mycorrhizal networks” (CMNs) which facilitate carbon and
63 nutrient transfer between organisms, beyond the immediate plant-fungus mutualism formed by
64 individuals. This relationship is often simplified to the mutual exchange of carbon-based
65 photosynthates for limiting soil nutrients that are more readily bioavailable to fungi (Smith &
66 Read, 2008), but is known to exist along a continuum from parasitic to mutualistic (Johnson *et*
67 *al.*, 1997; Klironomos, 2003; Mariotte *et al.*, 2013). A synthesis of empirical research at macro-
68 and micro-levels of ecological organization reveals a gap in understanding of structural and
69 functional properties that could predict how carbon and nutrients are transferred in CMNs (Silva
70 & Lambers, 2021).

71 The literature holds myriad and often complimentary, but sometimes contradictory,
72 hypotheses that could explain the CMN mutualism as a key structural and functional component
73 of ecosystems. For example, the “Wood Wide Web” hypothesis emerged from the analysis of
74 isotopically labeled carbon transferred between plants, presumably through fungal mycorrhizae.
75 Simard *et al.* (1997) concluded that plants that allocate carbon to sustain common fungal
76 symbionts also benefit from shared nutrients, while plants associating with mycorrhizal fungi
77 outside that network cannot. The “economics” hypothesis (Kiers *et al.*, 2011) proposes that
78 plants and fungi engage in “trades” of nutrients mined by fungi in exchange for plant
79 photosynthates (Fellbaum *et al.*, 2014; Werner & Dubbert, 2016; Averill *et al.*, 2019). In this
80 hypothesis, the terms of trade between plant and fungi are mediated by supply and demand for
81 limiting resources, which could create a dynamic market emerging from interactions between

82 environmental, biochemical, and biophysical variables. Complementing the economic analogy,
83 the “kinship” hypothesis proposes that phylogenetic distance within or across species promotes
84 functional gradients and preferential flow of resources in CMNs (Tedersoo *et al.*, 2020), in
85 which transfer of carbon and nutrients are predicted to be more frequent and abundant between
86 related individuals (e.g., seedlings and trees of the same species) than between unrelated
87 individuals (Pickles *et al.*, 2017).

88 The past two decades have seen extensive but inconclusive research on these hypotheses
89 and how they relate to empirical measurements of CMN structure and function. On the one hand,
90 economic analogies suggest that the reciprocally regulated exchange of resources between plants
91 and fungi in CMNs should favor the most beneficial cooperative partnerships (Kiers *et al.*, 2011;
92 Fellbaum *et al.*, 2014). On the other hand, reciprocal transfer is only found in a subset of
93 symbionts under specific conditions, while increased competition in CMNs is a more common
94 observation (Walder & van der Heijden, 2015; Weremijewicz *et al.*, 2016). At the core of this
95 controversy is whether CMNs actively support fungal growth at the expense of plant resource
96 demands (i.e., a fungi-centric view) or function as passive channels through which plants
97 regulate resource fluxes (i.e., a plant-centric view). If plant-centric, we expect to find that the
98 structure and functioning of CMNs give rise to consistent spatiotemporal patterns of resource
99 allocation akin to those predicted by the kinship hypothesis. If fungi-centric, we expect to find
100 that spatiotemporal patterns of resource allocation reflect the composition and functioning of the
101 fungal community regardless of the connecting plant nodes in CMNs. Data exist to support both
102 opposing views (see Silva & Lambers, 2021; Figueiredo *et al.*, 2021); therefore, we posit that
103 CMNs are neither plant- nor fungi-centric. Instead, perhaps rather than gregarious, AM fungi are
104 “agnostic” with respect to plant species composition and relatedness, and yet affected by major
105 plant functional traits that are known to influence resource use and allocation. There is no clear
106 evidence to suggest that AM fungi exhibit specificity for plant species as do host-specific
107 pathogens (Lee *et al.*, 2013). Even in the systems dominated by ectomycorrhizal (EM)
108 associations where most previous research into CMN structure and function was developed,
109 fungi tend to be generalists, although plant taxa-specific EM fungi occur at relatively high
110 proportion, especially in early successional temperate plant communities (McMahon *et al.*, 2022;
111 Spencer *et al.*, 2023). Building on previous research, our hypothesis represents a first-principles
112 simplification in which gradients in resource limitation, rather than species-specific plant-fungi

113 interactions, might allow us to better understand and predict the rates and direction of resource
114 transfer in CMNs.

115 To test the “agnostic fungi” hypothesis, we asked if interactions among biophysical and
116 biogeochemical processes could explain resource transfer in CMNs with more accuracy than
117 previous plant- or fungi-centric analogies. We studied how soil resource-use efficiency and plant
118 traits that are known to regulate physiological performance (Dawson *et al.*, 2022) and that are
119 expected to affect the transfer of carbon and nitrogen (Peaucelle *et al.*, 2019) in paired
120 experiments including restored prairie and pasture experimental sites under ambient conditions
121 and rain exclusion shelters (designed to affect soil water and nutrient mass flow). We replicated
122 our paired experimental setting at three different locations, with study sites distributed across a
123 520 km latitudinal gradient. Due to the climatically driven differences in communities across
124 sites, not all species were present at all sites (Table S1); however, all functional groups were
125 present at all sites and most species were present at more than one site. In this experiment, we
126 also sequenced strain-level variation in root fungal DNA, plant functional types, and leaf
127 stoichiometric traits to test if relatedness explained difference in resource transfer. This allowed
128 us to generalize our inferences about the structure and function of arbuscular CMNs in temperate
129 grasslands. The diversity of plants growth forms included in our study also affect CMN
130 composition and function. For example, Davison *et al.* (2020) found plant growth form altered
131 AM fungal community and functional diversity. Plant total biomass can also increase nitrogen
132 received through a CMN, an effect that may be compounded by whether plants are woody or
133 herbaceous (He *et al.*, 2019). This could be explained by larger or denser plants providing more
134 carbon. Both plants and fungi have economic spectra characterized by fast or slow traits and
135 nutrient strategies which together form an interacting continuum potentially driven by N
136 availability (Ward *et al.*, 2022). It is unclear to what extent plant or fungi characteristics drive
137 these plant-fungal interactions. Therefore, we designed an experiment to quantify how plant-
138 fungal interactions influence the structure and functioning of CMNs across broad environmental
139 gradients and resource constraints.

140

141 **Materials and Methods:**

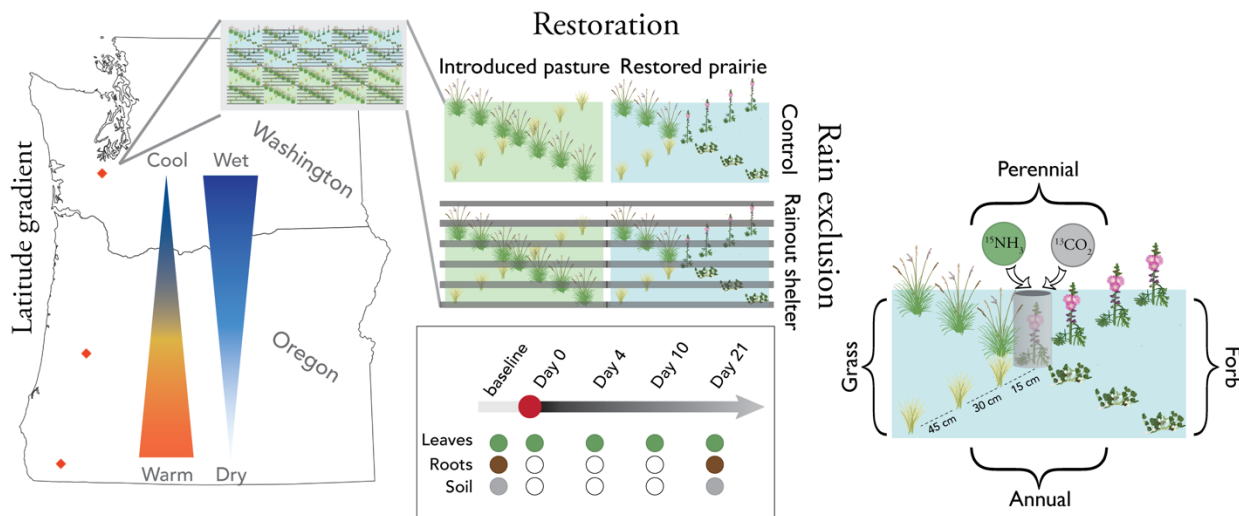
142 We conducted our experiment at three sites situated on a 520 km latitudinal transect that
143 spans three Mediterranean climates: cool, moist (northern site; Tenino, WA) to warm, moist

144 (central site; Eugene, OR) to warm, dry (southern site; Selma, OR). Each circular plot was 3 m in
145 diameter. Half of our plots were restored prairie systems (n = 10 per site) while the other half of
146 the plots had introduced pasture grasses established prior to restoration (n = 10 per site).
147 Restored prairie plots were mowed, raked, received herbicide, and seeded in 2014-2015,
148 followed by seeding in fall 2015, 2016, and 2017 (Reed *et al.*, 2019). We erected rainout shelters
149 that excluded 40% of the rainfall on half the plots at each site (n = 10 rain exclusion, 10 control
150 per site; Fig. 1).

151 All plants in our system have the potential to form associations with AM fungi (Table S1)
152 (Dickie *et al.*, 2013; Chaudhary *et al.*, 2016; Soudzilovskaia *et al.*, 2020). Previous work
153 demonstrated that the rainout shelters had minimal effects on aboveground community structure
154 or function (Dawson *et al.*, 2022), possibly due to the shoulder season effect of the
155 Mediterranean rain seasonality. This network of experimental sites was established in 2010 and
156 has been extensively studied since then (Reed *et al.*, 2019, 2021a,b,c; Peterson *et al.*, 2020)
157 including work on mycorrhizal fungi (Vandegrift *et al.*, 2015; Wilson *et al.*, 2016). Treatments
158 had marginal effects on the soil water potential (especially during the early growing season).
159 Pasture plots were dominated by one to a few species of introduced perennial grasses which we
160 targeted as donors in these plots. We used different species of perennial grass at each site. For
161 restored prairie plots, we targeted the native perennial forb *Sidalcea malviflora ssp. virgata*
162 common to ambient and drought treatments at all sites. Despite those differences, we did not find
163 significant changes in the average plant community composition or productivity under rain
164 exclusion, which also did not affect morphological and functional traits (e.g., specific leaf area,
165 iWUE, and C:N ratios) of the functional groups we selected for this experiment (Reed *et al.*,
166 2021c; Dawson *et al.*, 2022).

167 To test our new hypothesis, we built upon those preliminary data with a new dual isotope
168 label approach as follows. We labeled perennial plants central to each plot (hereafter, ‘donors’)
169 and monitored leaf ¹⁵N and ¹³C for the surrounding plants (‘receivers’) for up to 21 days. In
170 addition, we sampled roots and soils at 21 days post-labelling. We characterized AM fungal
171 DNA isolated from the root samples, as well as stable isotopes in all leaf and root samples. Our
172 experimental design was nested in a multi-year experiment where data loggers were used to
173 continuously measure temperature and moisture in all the manipulated plots.

174



175
176 **Figure 1. Schema of experimental set up, sampling, and effects of rainout shelters.**

177
178 *Isotopic labelling*

179 At each site, we selected a healthy perennial forb (*Sidalcea malviflora* ssp. *virgata* in
180 restored prairie plots [except in one plot where we used *Eriophyllum lanatum* due to a lack of *S.*
181 *malviflora* ssp. *virgata*]), or a perennial grass (*Alopecurus pratensis*, *Schedonorus arundinaceus*,
182 or *Agrostis capillaris*) in pasture plots at the center of each plot to receive the isotopic labels. On
183 sunny days between 11AM and 3PM at peak productivity for each site, we applied isotopically
184 enriched carbon (^{13}C) and nitrogen (^{15}N) as a pulse of carbon dioxide (CO_2) and ammonia (NH_3)
185 to the leaves of target “donor” species common across experimental sites. We performed the
186 labeling experiment using custom-made field-deployable clear chambers with internal fans built
187 to allow gas mixing and fast in situ assimilation of isotopic labels, following established
188 protocols developed in previous isotopically labeling studies (e.g., Silva *et al.*, 2015; Earles *et*
189 *al.*, 2016; Sperling *et al.*, 2017). We covered the donor plant with a clear plastic cylinder and
190 injected gas in sequence at 20-minute intervals. For $^{13}\text{CO}_2$, we made three injections of 2 mL
191 pure CO_2 (enriched at 98 atm % ^{13}C) to double the amount of CO_2 in the chamber each time. For
192 NH_3 , we made two injections of 10 mL pure NH_3 (98 atm% ^{15}N) at 20 minute intervals. The
193 dates of application were based on peak productivity estimated from Normalized Different
194 Vegetation Index (NDVI) at each site (see Reed *et al.*, 2019 for details). We sampled leaves from
195 each donor plant immediately after labeling (time point 0) as well as from all plants
196 approximately 4 days (time point 1), 10 days (time point 2), and 21 days (time point 3) post-
197 labelling as logistics permitted (Fig. 1, Table S2). We also collected leaves at time points 1, 2,

198 and 3 from up to twelve plants in each plot representing three replicates of factorial grass/forb
199 structural groups and annual/perennial life history strategies (Table S1). The number of plants
200 and represented groups depended on which plants were growing in each plot. For example,
201 pasture plots were limited to only grasses and the northern pasture plots had only perennial
202 grasses.

203 By applying enriched gases only to the aboveground portions of established perennial
204 donor plants, we introduced the isotopic tracer to both the plant and mycorrhizal fungal tissues
205 with minimal exposure of the soil to the tracers. At the end of the experiment, we harvested
206 entire plants and the soil surrounding the roots at time point 3 and kept them in cool conditions
207 until processing. We separated the roots and rhizospheres, and collected roots from each plant,
208 selecting approximately ten ~3 cm fine root fragments per sample (i.e., third order or finer,
209 where available) for DNA extraction and identification. All roots and rhizosphere soils were
210 stored at -80° C until processing.

211

212 *Baseline and Resource Transfer Calculations*

213 Before isotopic labeling, we collected soil, leaves, and roots from each site. We collected
214 soils in late spring and early summer 2019 to 20 cm depth in each plot. From these soil samples,
215 we removed root fragments that represented the typical roots seen in each plot. We collected
216 leaves for each species in each plot; however, these leaves were contaminated with ¹⁵N during
217 transport. To replace contaminated samples, we separately sampled leaves from biomass
218 samplings collected in late spring and early summer 2019, ensuring that annual and perennial
219 grasses and forbs were represented at each site.

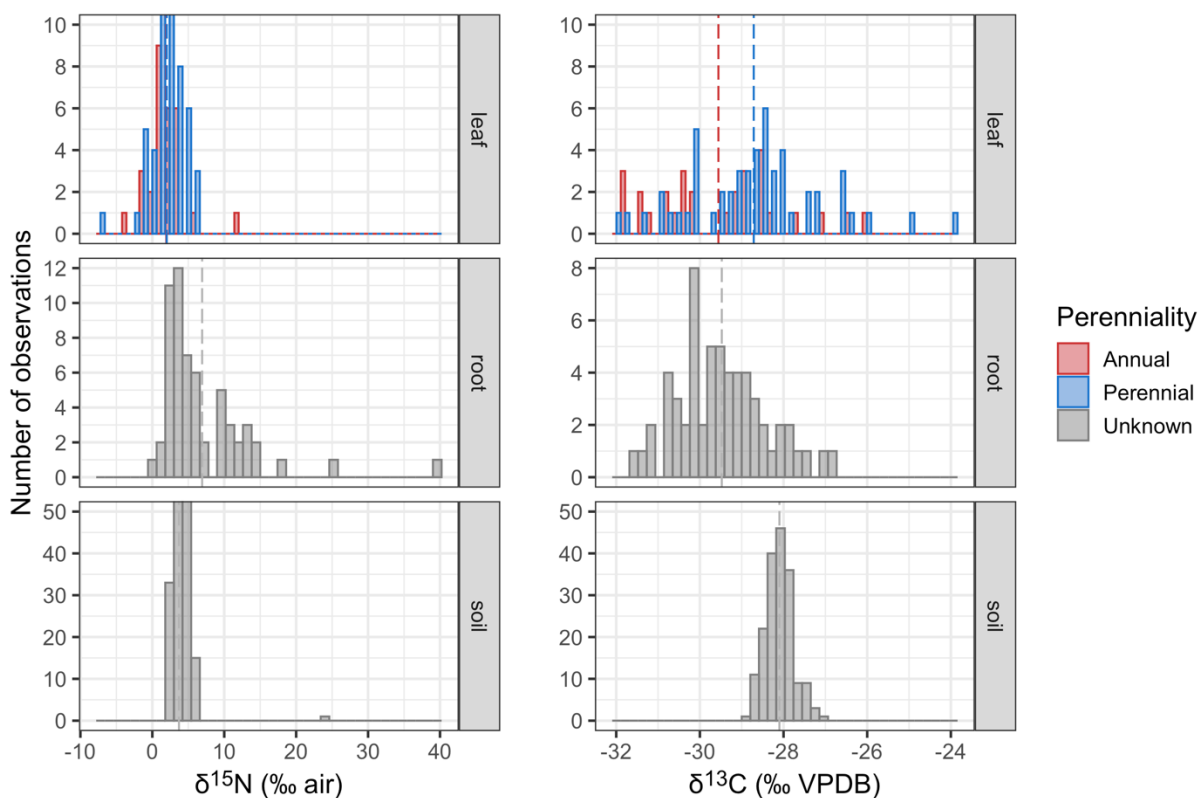
220 We oven-dried all samples at 65° C to constant mass and encapsulated them for stable
221 isotope analysis. All stable isotope analysis was done at UC Davis Stable Isotope Facilities using
222 an Elementar Vario EL Cube or Micro Cube elemental analyzer (Elementar Analysensysteme
223 GmbH, Hanau, Germany) interfaced to a PDZ Europa 20-20 isotope ratio mass spectrometer
224 (Sercon Ltd., Cheshire, UK). We calculated the amount of carbon and nitrogen in each plant
225 compartment (leaves and roots) using standard label recovery equations (Silva *et al.*, 2015),
226 using baseline values measured before application of the labelled gases to capture background
227 variations in isotopic composition of unenriched leaves, roots, and soil samples

228 At each relevant point in space and time, we calculated % nitrogen and % carbon derived from
229 label (%NDFL and %CDFL, respectively) as follows (Kramer *et al.*, 2002; He *et al.*, 2009; Silva
230 *et al.*, 2015).

231 **Equation 1**

$$\frac{atm\%_{post-label} - atm\%_{baseline}}{atm\%_{labelling\ gas}}$$

233 Baseline values were calculated from the site- and annual/perennial-specific values for each plant
234 material. Site-specific baseline soil and root isotope ratios represent the whole community
235 because of interconnected rhizospheres where it was not possible to identify specific species.
236 In all cases, baseline values fell within the expected range for our region (Fig. 2). We calculated
237 intrinsic water-use efficiency following Farquhar and Richards (1984) using the baseline ^{13}C
238 values from the original samples because the contamination only occurred with ^{15}N .



239
240 **Figure 2. Natural abundance of stable isotopes in leaves, roots, and soil before labelling.**
241 Dashed lines indicate mean value.
242

243 To better understand post-labelling soil enrichment, we selected a subset of rhizosphere
244 soils that represented six donor plants at each site divided equally between restored prairie and
245 pasture plots, and selected the three most highly ¹⁵N enriched interspecific receivers in each plot
246 across the sites. In addition, we sampled three most highly enriched interspecific receivers at
247 each site and restored prairie-introduced pasture combination (if they had not been sampled
248 previously). Because pasture plots were sometimes monodominant grasses, we sampled the top
249 three enriched intraspecific receivers at each site and treatment. In total, this came to 48 post-
250 labelling soil samples in 29 plots.

251

252 *Fungal analysis*

253 We extracted DNA from roots of 450 plants harvested at time point 3 (21 days post-label)
254 using Qiagen DNeasy Powersoil HTP kits (Qiagen, Hilden, Germany). We only analyzed DNA
255 from roots, not from the soils collected from each plant's rhizosphere. We characterized each
256 sample's AM fungal composition with a two-step PCR protocol that amplified a ~550bp
257 fragment of the SSU rRNA gene (the most well-supported region for AM fungal taxonomic
258 resolution (Dumbrell *et al.*, 2011). We used WANDA (5'- CAGCCGCGGTAATTCCAGCT- 3')
259 and AML2 (5'- GAACCCAAACACTTTGGTTTCC-3') primers (Lee *et al.*, 2008; Langmead &
260 Salzberg, 2012). We used primers with unique indices so we could multiplex several projects on
261 a single run. We quantified successful PCR amplicons with the Quant-iT PicoGreen dsDNA
262 Assay Kit (Invitrogen, Waltham, MA, USA) on a SpectraMax M5E Microplate Reader
263 (Molecular Devices, San Jose, CA, USA) before purifying with QIAquick PCR Purification kits
264 (Qiagen). We sequenced the purified pools on the Illumina MiSeq platform (paired-end 300bp,
265 Illumina Inc., San Diego, CA, USA) at the University of Oregon Genomics and Cell
266 Characterization Core Facility (Eugene, OR, USA). Reads were deduplicated with UMI-tools
267 using unique molecular identifiers (UMIs) inserted during PCR (Smith *et al.*, 2017).

268 We assigned amplicon sequence variants (ASVs) using the dada2 pipeline with standard
269 quality filtering and denoising parameters (Callahan *et al.*, 2016). The dada2 pipeline maintains
270 strain-level diversity at the scale of individual sequence variants rather than clustering sequences
271 into OTUs. This fine-scale measure of fungal sequence diversity was particularly important for
272 our analyses to maintain the greatest chance of detecting a single AM fungal 'individual' in
273 multiple plant root samples. Taxonomy was assigned to ASVs using the MaarjAM database

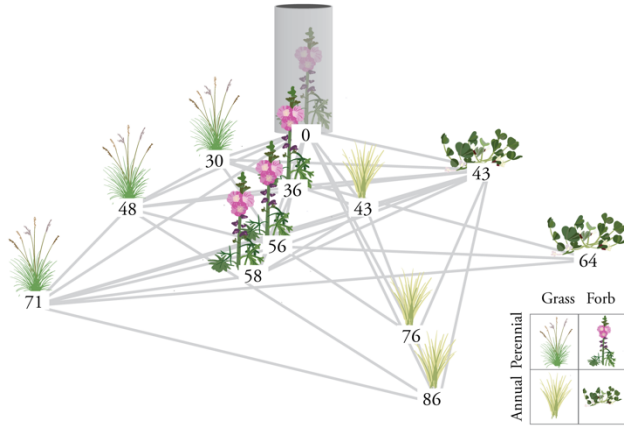
274 (2019 release) (Öpik *et al.*, 2010). We used a Bayesian mixture model in the DESeq2 package
275 (Love *et al.*, 2014) to scale ASV counts within and across samples to avoid artificial taxon
276 abundance biases (Anders & Huber, 2010).

277

278 *Data analysis*

279 We performed all analyses in R ver. 4.0.4 (R Core team, 2015). We removed one plant
280 with ¹⁵N outlier data. We also removed five mislabeled samples. To meet statistical assumptions,
281 we only included data from plants with successful root fungal DNA extraction. In total, we
282 analyzed data from 389 unique plants: 53 donors and 336 receivers.

283 We tested the relationship between NDFL and plant traits (grass/forb, annual/perennial,
284 iWUE, C:N, degrees of connectivity, interaction term between grass/forb and annual/perennial)
285 and site conditions (position on latitude gradient, pasture/restored, rain exclusion treatment,
286 distance from donor, time from labelling) with a mixed-effect ANOVA (plot as random effect;
287 Table 1). We constructed a phyloseq object using the ASV table with normalized counts
288 (McMurdie and Holmes 2013), and used iGraph, metagMisc, and RCy3 (Nepusz and Csardi
289 2006, Mikryukov 2017, Gustavsen *et al.* 2019) to create networks for each plot. In each network,
290 nodes represented individual plants and edges between nodes represent plants sharing at least
291 one fungal DNA sequence variant. The weighted edges are based on how many fungal ASVs
292 were shared among plants. We calculated degrees of connectivity with tidygraph (Petersen,
293 2022) to examine how many plants each individual plant was ‘connected’ to (by means of shared
294 fungal ASVs) in each plot (Fig. 3). We also calculated whether each receiver plant shared fungal
295 ASVs with the central donor plant in each plot. We visualized individual plot networks in
296 CytoScape. We visualized shifts in AM fungal community composition using non-metric multi-
297 dimensional scaling (NMDS) in the vegan package, demonstrating the AM fungal community
298 similarity across plants (Oksanen *et al.*, 2022).



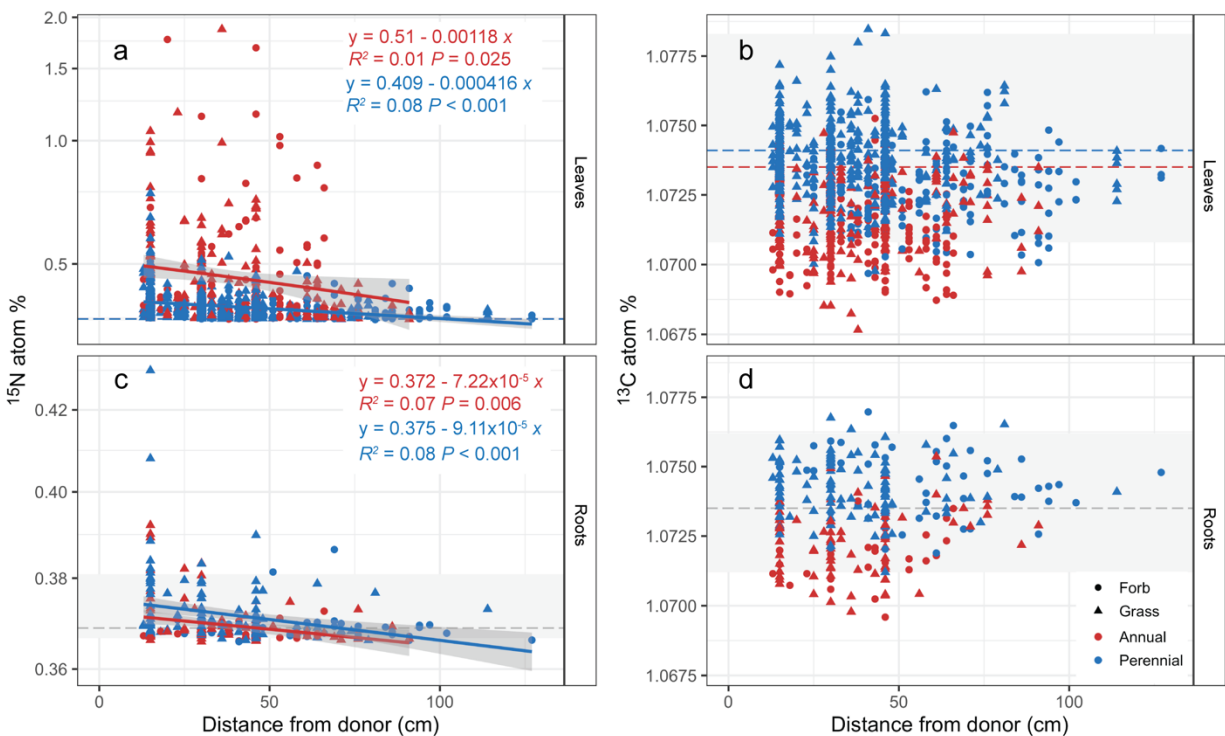
299

300 **Figure 3. Example of how networks were constructed for each plot.** The grey cylinder
301 indicates the donor plant for the plot. Numbers beneath the receivers are the distance (in
302 centimeters) from the donor. Degrees were calculated as how many plants each individual plant
303 was connected to by shared fungal ASVs; for example, the perennial grass at 71 cm has 7
304 degrees.

305

306 **Results:**

307 Assimilation of isotopic tracers was similar between labeled “donor” plants with no
308 significant differences on average between sites or experimental treatments within sites,
309 including rainfall exclusion or restored status (Fig. S1). At all sites, foliar assimilation of ^{15}N and
310 ^{13}C by donor plants led to enrichment levels ranging from approximately 5-10 fold higher than
311 baselines, with only a few that were less than 2-fold from baseline. Foliar enrichment levels
312 decreased consistently at all sites and treatments over the 21 day sampling period. We found
313 significant spatial and temporal differences in foliar and root isotope ratios in donors and
314 receivers resulting from interspecific transfer of carbon and nitrogen (Fig. 4; Table 1). Receiver
315 foliar enrichment levels did not correlate with donor foliar enrichment levels within the same
316 plot (Fig. S2).



317

318 **Figure 4. Decreased receiver enrichment with distance from donor in leaves and roots.**

319 Dashed lines indicate natural abundance means; grey boxes indicate range of natural abundance

320 variation shown in Fig. 2. There is no systematic enrichment of ^{13}C ; however, there is high ^{15}N

321 enrichment in leaves. Y-axes are log₁₀ scale. Note that the y-axis scales are different between ^{15}N

322 leaves and ^{15}N roots. See Fig. S3 for boxplots of enrichment data by grass/forb and

323 annual/perennial.

324 **Table 1. ANOVA results effects on nitrogen derived from label (NDFL).** Carbon was not
325 enriched so carbon derived from label was not tested.

| | χ^2 | P-value |
|------------------------------------------------|----------|------------------|
| <i>Fixed effects</i> | | |
| Annual/perennial | 37.895 | <0.001 |
| Grass/forb | 19.075 | <0.001 |
| iWUE | 0.150 | 0.698 |
| Degree of connectivity | 0.847 | 0.357 |
| C:N | 77.547 | <0.001 |
| Site | 4.913 | 0.086 |
| Drought treatment | 0.189 | 0.664 |
| Restoration treatment | 2.398 | 0.121 |
| Distance from donor | 15.423 | <0.001 |
| Time from labelling | 162.582 | <0.001 |
| Annual/perennial:Grass/forb interaction | 8.670 | 0.003 |
| <i>Random effect</i> | | |
| Plot | | <0.001 |

326
327 Allocation of ^{13}C and ^{15}N tracers to roots and subsequent transfer to “receiver” species
328 did not follow expected patterns (e.g., despite donors being perennial, annual receivers were
329 more enriched, indicating that relatedness did not drive the transfer, Fig. 4, Table 1). Allocation
330 and transfer varied significantly between functional groups due to their intrinsic differences in
331 tissue stoichiometry (Table 1). We selected 18 common annual/perennial and grass/forb species
332 of receiver plants, which revealed significant differences between functional groups for NDFL
333 (Fig. 5) but no detectable CDFL relative to baseline (Fig. 4). Rain exclusion treatment,

334 restoration treatment, and site did not affect interspecific transfer of nitrogen (Fig S4; ANOVA,
 335 $P > 0.05$, Table 1), and carbon was not enriched enough to test transfer (Fig. 4). We did,
 336 however, observe significant differences in nitrogen transfer by functional group (Table 1),
 337 mirroring intrinsic differences in tissue stoichiometry and iWUE (Fig. 5), despite no significant
 338 enrichment in soils collected from the rhizosphere of those same plants (Fig. S5). We also found
 339 that C:N affected NDFL, although not in a simple linear manner as shown by the ANOVA
 340 (Table 1), and with no apparent correlation between NDFL and iWUE (Fig. 5). We did detect a
 341 low level of soil enrichment in 4 out of 23 donor soil samples (ranging from 0.382 to 0.479
 342 atm% ^{15}N).

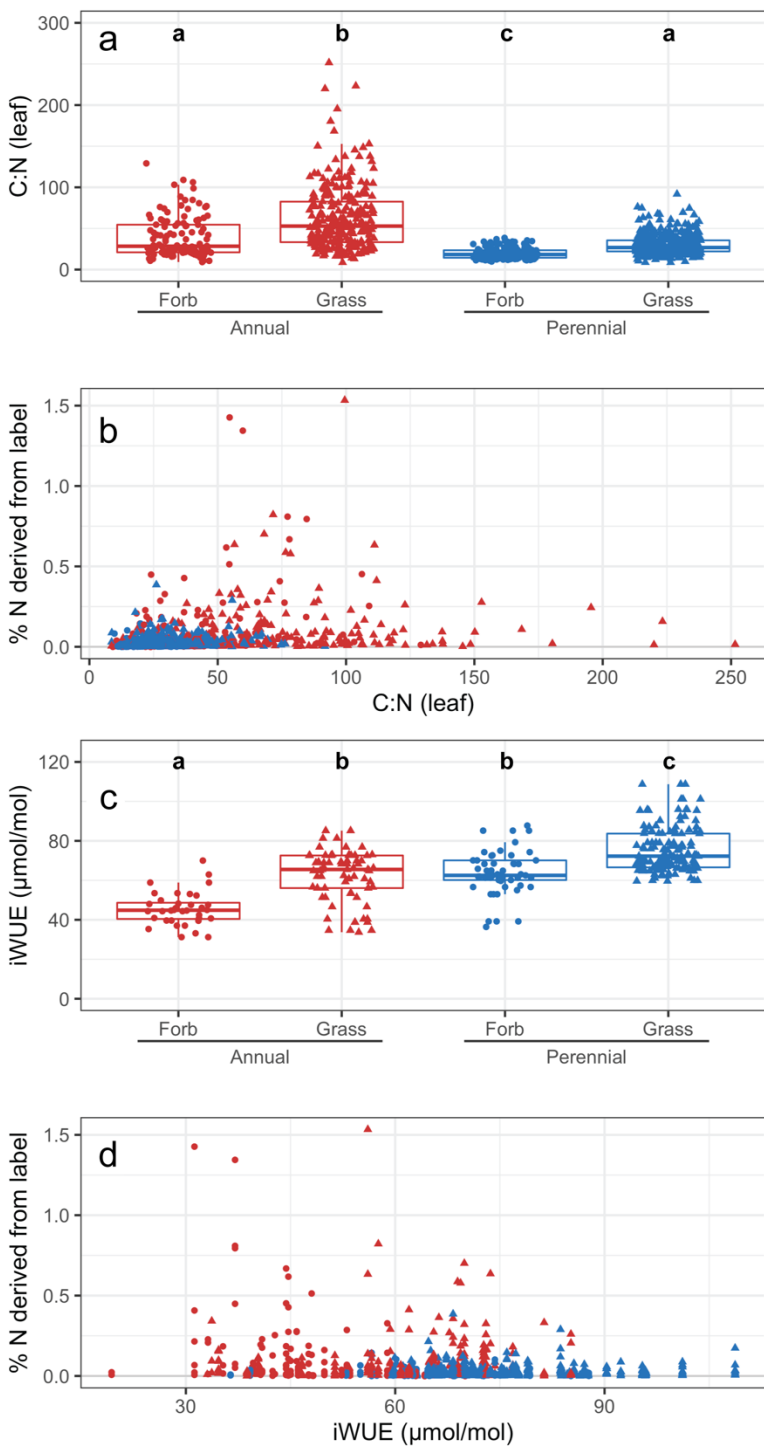
343 Annuals had greater ^{15}N foliar enrichment compared to perennials (ANOVA, $P < 0.001$,
 344 Tables 1 and 2). Foliar enrichment decreased over both time and space (ANOVA $P < 0.001$; Fig.
 345 4, Fig. S1). On average, annuals had a lower leaf nitrogen content and higher C:N than
 346 perennials (Table 2, Fig. 5). Forbs had higher NDFL than grasses (ANOVA, $P < 0.001$, Table 1)
 347 as well as a lower C:N. There was a significant interaction between annual/perennial and
 348 grass/forb form (ANOVA, $P = 0.003$, Table 1).

349

350 **Table 2. Nitrogen derived from label (NDFL) and leaf tissue nitrogen (% N) four days after**
 351 **labeling.**

| | | <i>n</i> | NDFL | | | | | % N | | | | |
|-----------|-------|----------|-------------|-------|-----------|------------|------------|-------------|-------|-----------|------------|------------|
| | | | <i>Mean</i> | \pm | <i>SD</i> | <i>Min</i> | <i>Max</i> | <i>Mean</i> | \pm | <i>SD</i> | <i>Min</i> | <i>Max</i> |
| Annual | Forb | 54 | 0.206 | \pm | 0.281 | 0.003 | 1.427 | 1.731 | \pm | 0.849 | 0.528 | 4.081 |
| | Grass | 93 | 0.130 | \pm | 0.199 | 0.001 | 1.534 | 1.233 | \pm | 0.919 | 0.359 | 8.004 |
| Perennial | Forb | 67 | 0.033 | \pm | 0.026 | 0.006 | 0.144 | 2.521 | \pm | 0.753 | 1.079 | 4.136 |
| | Grass | 148 | 0.040 | \pm | 0.028 | 0.005 | 0.147 | 1.600 | \pm | 0.529 | 0.614 | 2.938 |

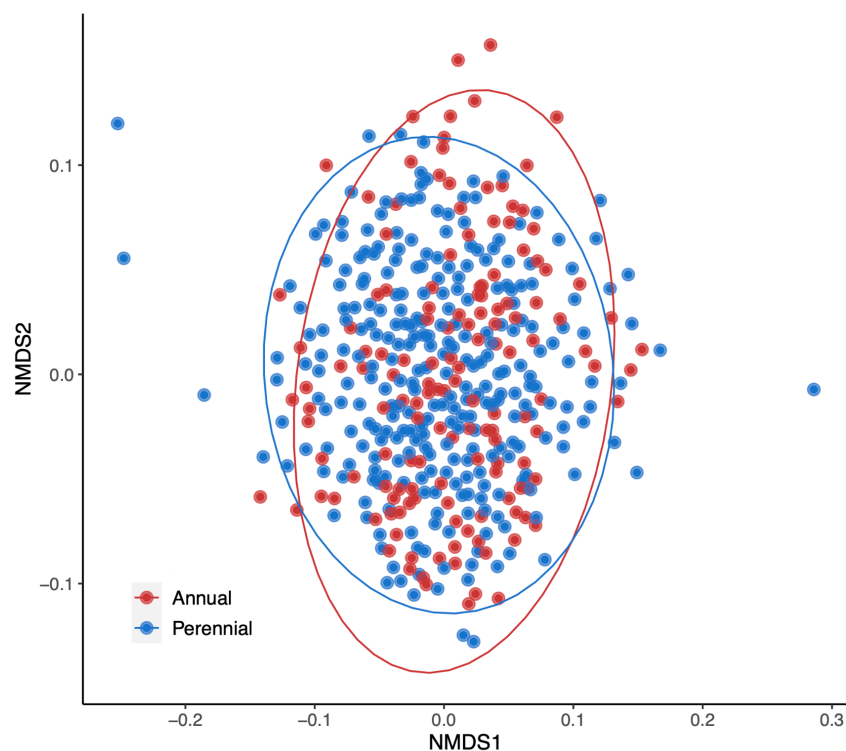
352



353
354 **Figure 5. Stoichiometric and functional traits compared to nitrogen derived from transfer.**
355 A) Leaf C:N by annual/perennial. B) Percent ^{15}N derived from label (DFL) compared to C:N in
356 leaves. C) iWUE by annual/perennial as measured before labelling. D) Percent ^{15}N DFL

357 compared to iWUE in leaves at all time points. Letters above boxplots indicate significant
358 differences.

359
360 Our analysis of fungal community composition shows a high degree of connectivity
361 between plants of different species but no obvious pattern of connectedness that could explain
362 preferential nutrient transfer by plant functional groups. We found that $97.25\% \pm 8.01$ (SD) of
363 all plants roots within each experimental plot shared at least one fungal DNA sequence variant
364 (ASV) with another plant of the same plot. Fungal community composition was similar across
365 plant functional groups (Fig. 6, PERMANOVA pseudo-F statistic = 2.269, $R^2 = 0.005$, $p =$
366 0.001). Annual plants shared fungi with more plants in the same plot (4.74 plants ± 2.62 SD)
367 compared to perennials (4.04 plants ± 2.49 SD ; t-test, $P = 0.019$; Table S3), but degrees of
368 connectivity did not predict nitrogen transfer (Table 1). Seventy-three percent of plants were
369 colonized by four or fewer fungi and shared fungi with five or fewer other plants in the plot,
370 making it difficult to determine if strength of connectivity altered nitrogen transfer (Fig. S6).



371
372 **Figure 6. NMDS of fungal communities.** Each point represents an individual plant ordinated by
373 the Bray Curtis dissimilarities for AM fungal composition. PERMANOVA pseudo-F statistic =
374 2.269, $R^2 = 0.005$, $p = 0.001$.

375

376 **Discussion:**

377 In our extensively replicated spatiotemporal isotopic tracer experiment, the assimilation
378 and allocation of limiting resources in CMNs was neither plant- nor fungi-centric. Our data show
379 that AM fungi are “agnostic” with respect to plant species composition and relatedness, and that
380 the transfer of nitrogen (an important nutrient that can limit plant growth in our system) is
381 regulated by major functional traits that are known to influence resource use and allocation in
382 plant communities. The rates and direction of resource transfer in CMNs, inferred from pulse
383 labeling and recovery of ^{15}N in leaves and rhizospheres, can be predicted from leaf C:N and
384 distance from donor species (Fig 1). Across all sites and treatments, we observed a stronger sink
385 for ^{15}N in annual plants close to the source donor, indicating preferential transfer of limiting
386 resources to that functional group of plants. This observation is contrary to the expectation of the
387 kinship hypothesis that preferential transfer would be expected to occur from a perennial donor
388 to a perennial receiver. Although plants shared a high proportion of fungal ASVs in their roots
389 (Fig. 6), connectivity did not predict ^{15}N transfer (Table 1), and thus we found no evidence for a
390 fungi-centric hypothesis based on which all connected plants would have been expected to be
391 equally enriched in ^{15}N . Our data suggest that rates and direction of resource transfer in CMNs
392 reflect plant nutrient requirements and spatial proximity.

393 We designed this experiment to be informed by previous hypotheses on how carbon and
394 nitrogen transfer occurs in highly connected CMNs, where a dilution of the applied ^{13}C label is
395 to be expected given the vast amounts of carbon in the soil and plant biomass. We conducted
396 repeated spatiotemporal sampling of isotopic enrichment levels at increasing distances from
397 donor species, days to weeks after labelling, and in well-established communities exposed to
398 multiple years of experimental treatments, expecting to find evidence of kinship (i.e., greatest
399 resource transfer in related plants), driven by CMN economics (i.e., ^{15}N transfer rates coinciding
400 with ^{13}C investment in root and fungal mass). Our donor plants were perennials while annuals
401 received, on average, an order of magnitude higher enrichment. Thus, we discarded kinship as a
402 possible driver of transfer in this system. We also did not find evidence of a relationship between
403 ^{15}N in leaves and ^{13}C in roots because we did detect ^{15}N enrichment in leaves but no ^{13}C
404 enrichment in roots. We did, however, find significant ^{13}C enrichment in the donor plants.
405 Therefore, our data do not support either hypothesis, and instead suggest AM fungi are

406 “agnostic” with respect to plant species partnerships, forming CMNs where the rates and
407 direction of resource transfer ultimately reflects a sink-source strength effects, consistent with
408 previous observations of stoichiometric source-sink manipulations of carbon and nitrogen within
409 plants (Ruiz-Vera *et al.*, 2017; Tegeder & Masclaux-Daubresse, 2018; Cai *et al.*, 2021), but in
410 our case observed at the community scale.

411 Nitrogen enrichment levels remained high in leaves and many roots at the end of the
412 experiment, allowing us to measure NDFL across the community and infer the main drivers of N
413 transfer. However, carbon enrichment levels faded before plants were harvested approximately
414 21 days post-labelling, either due to losses via respiration or redistribution in CMNs where it
415 became undetectable in all but a few cases. After controlling for variation in assimilation rates by
416 calculating NDFL, we found that annual plants received greater ^{15}N enrichment than perennial
417 plants. Plants closest to the donor were most enriched, and ^{15}N enrichment decreased over time
418 (Fig. 4). Plant connectivity through an assumed CMN did not predict ^{15}N enrichment. Although
419 the rainout shelters had limited effect, there were major differences across the latitudinal gradient
420 represented by the sites in temperature and soil moisture availability (Reed *et al.*, 2019; Dawson
421 *et al.*, 2022); however, neither treatment nor site affected our results.

422 The major drivers of differences in allocation of ^{13}C and ^{15}N to roots and subsequent
423 transfer to “receiver” species were the intrinsic difference in plant functional types and correlated
424 traits, including measured leaf C:N. Previous studies in northern California under environmental
425 conditions similar to those found in our southernmost experimental site showed rapid (days to
426 weeks) transfer of ^{15}N applied to the leaves of ectomycorrhizal pines to surrounding annual AM
427 plant receivers (He *et al.*, 2006). Those results were interpreted as evidence for agnostic CMNs
428 because “direct fungal connections are not necessary for N transfer among plants” and “leaves of
429 the annual plants had greater ^{15}N derived from source and were more enriched (^{15}N at % excess
430 and $\delta^{15}\text{N}$ values) than perennial receivers, irrespective of the mycorrhizal type.” Similarly, as
431 proposed by He *et al.* (2006), our observation of agnostic ^{15}N transfer from donor to receivers
432 suggests that annual plants were a strong sink for N which could be explained by stoichiometric
433 gradients that affect root exudation and recapture of N-containing materials from rhizodeposition
434 (Høgh-Jensen & Schjoerring, 2001; Mayer *et al.*, 2003). Our data corroborate rapid agnostic
435 transfer among AM plants, with no detectable enrichment in root or soil ^{13}C near roots 21 days

436 post-labelling, but do not allow us to determine general mechanisms that are responsible for the
437 ^{15}N transfers.

438 We inferred a high connectivity between plants within each given treatment and site
439 given the highly similar fungal composition in the root systems of both perennial and annual
440 plants (Fig. 6). Given the constraints of ASV-identified data, we did this analysis on a strain-
441 level scale and it is possible that separate spores of the same ASV separately infected plants
442 within the same plot. However, we are reasonably confident in our use of fungal ASVs as a
443 proxy for connectivity given the strong overlap in our community and because individuals of one
444 ASV can anastomose in the soil (Mikkelsen *et al.*, 2008). This overlap could explain the lack of
445 support for the kinship hypothesis in our dataset and offers further support for stoichiometric
446 gradients in general, and C:N gradients in particular, as a principal control of terms of trade in
447 CMNs (Kiers *et al.*, 2011).

448 We found that plant-soil stoichiometric gradients and functional traits were the strongest
449 drivers of resource sharing in grassland CMNs. We interpret this finding as evidence of
450 biochemical and biophysical sinks, in which nutrients are allocated to plants with the greatest
451 need for those nutrients, either through a ‘passive’ mycorrhizal network or direct uptake from
452 soil, or that nutrients should be allocated through water flow. Expanding on previous studies, we
453 propose that agnostic AM fungi facilitate spatiotemporal dynamics of carbon and nitrogen
454 transfer through CMNs in ways that are neither plant- nor fungi-centric. That is, plants and fungi
455 that are located closer together in space and with stronger demand for resources over time are
456 more likely to receive larger amounts of those limiting resources.

457

458 **Acknowledgements:**

459 The authors thank the Siskiyou Field Institute, The Nature Conservancy, and Capitol Land Trust
460 for providing sites for this experiment, Laurel Pfeifer-Meister, Bitty Roy, Bart Johnson, Graham
461 Bailes, Aaron Nelson, and Matthew Krna for their contributions to experimental design, Emily
462 Scherer for her assistance with sample analysis, Bitty Roy and Leonel Sternberg for comments
463 on the manuscript, and numerous others for assistance with the HOPS project. This experiment
464 was funded by National Science Foundation Macrosystems Biology grant #1340847, Plant Biotic
465 Interactions grant #1758947, and Convergence Accelerator Pilot grant #1939511.

466

467 **Competing interests:**

468 The authors have no competing interests to declare.

469 **Author contributions:**

470 L.C.R.S, S.D.B., and B.J.M.B. designed the research; H.R.D., K.L.S., T.M.M., B.B., and P.B.R.
471 performed the research; H.R.D. led the data analysis and manuscript preparation with K.L.S.
472 assisting; all authors contributed to revising the manuscript and approved the publication.

473

474 **Data availability:**

475 Data used in these analyses are available online at the Data Dryad repository
476 (<https://doi.org/10.5061/dryad.7pvmcvdxt>).

477

478 **References:**

479 **Anders S, Huber W. 2010.** Differential expression analysis for sequence count data. *Genome*
480 *Biology* **11**: 1–12.

481 **Averill C, Bhatnagar JM, Dietze MC, Pearse WD, Kivlin SN. 2019.** Global imprint of
482 mycorrhizal fungi on whole-plant nutrient economics. *Proceedings of the National Academy of*
483 *Sciences of the United States of America* **116**: 23163–23168.

484 **Brundrett MC. 2009.** Mycorrhizal associations and other means of nutrition of vascular plants:
485 understanding the global diversity of host plants by resolving conflicting information and
486 developing reliable means of diagnosis. *Plant and Soil* **320**: 37–77.

487 **Cai Z, Xie T, Xu J. 2021.** Source–sink manipulations differentially affect carbon and nitrogen
488 dynamics, fruit metabolites and yield of Sacha Inchi plants. *BMC Plant Biology* **21**: 1–14.

489 **Callahan BJ, McMurdie PJ, Rosen MJ, Han AW, Johnson AJA, Holmes SP. 2016.** DADA2:
490 High-resolution sample inference from Illumina amplicon data. *Nature Methods* **2016 13:7 13**:
491 581–583.

492 **Chaudhary VB, Rúa MA, Antoninka A, Bever JD, Cannon J, Craig A, Duchicela J, Frame**
493 **A, Gardes M, Gehring C, et al. 2016.** Data Descriptor: MycoDB, a global database of plant
494 response to mycorrhizal fungi. *Nature*: 3:160028.

495 **Davison J, García de León D, Zobel M, Moora M, Bueno CG, Barceló M, Gerz M, León D,**
496 **Meng Y, Pillar VD, et al. 2020.** Plant functional groups associate with distinct arbuscular
497 mycorrhizal fungal communities. *New Phytologist* **226**: 1117–1128.

- 498 **Dawson HR, Maxwell TM, Reed PB, Bridgham SD, Silva LCR. 2022.** Leaf traits predict
499 water-use efficiency in U.S. Pacific Northwest grasslands under rain exclusion treatment.
500 *Journal of Geophysical Research: Biogeosciences* **127**: e2022JG007060.
- 501 **Dickie IA, Martínez-García LB, Koele N, Grelet GA, Tylianakis JM, Peltzer DA,**
502 **Richardson SJ. 2013.** Mycorrhizas and mycorrhizal fungal communities throughout ecosystem
503 development. *Plant and Soil* **367**: 11–39.
- 504 **Dumbrell AJ, Ashton PD, Aziz N, Feng G, Nelson M, Dytham C, Fitter AH, Helgason T.**
505 **2011.** Distinct seasonal assemblages of arbuscular mycorrhizal fungi revealed by massively
506 parallel pyrosequencing. *New Phytologist* **190**: 794–804.
- 507 **Earles JM, Sperling O, Silva LCR, McElrone AJ, Brodersen CR, North MP, Zwieniecki**
508 **MA. 2016.** Bark water uptake promotes localized hydraulic recovery in coastal redwood crown.
509 *Plant, Cell & environment* **39**: 320–328.
- 510 **Farquhar GD, Richards RA. 1984.** Isotopic Composition of Plant Carbon Correlates With
511 Water-Use Efficiency of Wheat Genotypes. *Functional Plant Biology* **11**: 539–552.
- 512 **Fellbaum CR, Mensah JA, Cloos AJ, Strahan GE, Pfeffer PE, Kiers ET, Bücking H. 2014.**
513 Fungal nutrient allocation in common mycorrhizal networks is regulated by the carbon source
514 strength of individual host plants. *New Phytologist* **203**: 646–656.
- 515 **Figueiredo AF, Boy J, Guggenberger G. 2021.** Common Mycorrhizae Network: A Review of
516 the Theories and Mechanisms Behind Underground Interactions. *Frontiers in Fungal Biology* **0**:
517 48.
- 518 **Gustavsen JA, Pai S, Isserlin R, Demchak B, Pico AR. 2019.** RCy3: Network biology using
519 Cytoscape from within R. *F1000Research* **8**: 1774.
- 520 **He X, Bledsoe CS, Zasoski RJ, Southworth D, Horwath WR. 2006.** Rapid nitrogen transfer
521 from ectomycorrhizal pines to adjacent ectomycorrhizal and arbuscular mycorrhizal plants in a
522 California oak woodland. *New Phytologist* **170**: 143–151.
- 523 **He Y, Cornelissen JHC, Wang P, Dong M, Ou J. 2019.** Nitrogen transfer from one plant to
524 another depends on plant biomass production between conspecific and heterospecific species via
525 a common arbuscular mycorrhizal network. *Environmental Science and Pollution Research* **26**:
526 8828–8837.
- 527 **He X, Xu M, Qiu GY, Zhou J. 2009.** Use of ¹⁵N stable isotope to quantify nitrogen transfer
528 between mycorrhizal plants. *Journal of Plant Ecology* **2**: 107–118.

- 529 **van der Heijden MGA, Martin FM, Selosse MA, Sanders IR. 2015.** Mycorrhizal ecology and
530 evolution: the past, the present, and the future. *New Phytologist* **205**: 1406–1423.
- 531 **Høgh-Jensen H, Schjoerring JK. 2001.** Rhizodeposition of nitrogen by red clover, white clover
532 and ryegrass leys. *Soil Biology and Biochemistry* **33**: 439–448.
- 533 **Johnson NC, Graham JH, Smith FA. 1997.** Functioning of mycorrhizal associations along the
534 mutualism–parasitism continuum. *New Phytologist* **135**: 575–585.
- 535 **Kenrick P, Strullu-Derrien C. 2014.** The Origin and Early Evolution of Roots 1. *Plant*
536 *Physiology*: 570–580.
- 537 **Kiers ET, Duhamel M, Beesetty Y, Mensah JA, Franken O, Verbruggen E, Fellbaum CR,**
538 **Kowalchuk GA, Hart MM, Bago A, et al. 2011.** Reciprocal rewards stabilize cooperation in
539 the mycorrhizal symbiosis. *Science* **333**: 880–882.
- 540 **Klironomos JN. 2003.** Variation in plant response to native and exotic arbuscular mycorrhizal
541 fungi. *Ecology* **84**: 2292–2301.
- 542 **Kramer AW, Doane TA, Horwath WR, Kessel C van. 2002.** Combining fertilizer and organic
543 inputs to synchronize N supply in alternative cropping systems in California. *Agriculture,*
544 *Ecosystems & Environment* **91**: 233–243.
- 545 **Langmead B, Salzberg SL. 2012.** Fast gapped-read alignment with Bowtie 2. *Nature Methods*
546 *2012 9:4 9*: 357–359.
- 547 **Lee E-H, Eo J-K, Ka K-H, Eom A-H. 2013.** Mycobiology diversity of arbuscular mycorrhizal
548 fungi and their roles in ecosystems. **41**: 121–125.
- 549 **Lee J, Lee S, Young JPW. 2008.** Improved PCR primers for the detection and identification of
550 arbuscular mycorrhizal fungi. *FEMS Microbiology Ecology* **65**: 339–349.
- 551 **Love MI, Huber W, Anders S. 2014.** Moderated estimation of fold change and dispersion for
552 RNA-seq data with DESeq2. *Genome Biology* **15**: 1–21.
- 553 **Mariotte P, Meugnier C, Johnson D, Thébault A, Spiegelberger T, Buttler A. 2013.**
554 Arbuscular mycorrhizal fungi reduce the differences in competitiveness between dominant and
555 subordinate plant species. *Mycorrhiza* **23**: 267–277.
- 556 **Mayer J, Buegger F, Jensen ES, Schloter M, Heß J. 2003.** Estimating N rhizodeposition of
557 grain legumes using a ¹⁵N in situ stem labelling method. *Soil Biology and Biochemistry* **35**: 21–
558 28.

- 559 **McMahen K, Guichon SHA, Anglin CD, Lavkulich LM, Grayston SJ, Simard SW. 2022.**
560 Soil microbial legacies influence plant survival and growth in mine reclamation. *Ecology and*
561 *Evolution* **12**: e9473.
- 562 **McMurdie PJ, Holmes S. 2013.** phyloseq: An R Package for Reproducible Interactive Analysis
563 and Graphics of Microbiome Census Data. *PLOS ONE* **8**: e61217.
- 564 **Mikkelsen BL, Rosendahl S, Jakobsen I. 2008.** Underground resource allocation between
565 individual networks of mycorrhizal fungi. *New Phytologist* **180**: 890–898.
- 566 **Mikryukov V. 2017.** metagMisc.
- 567 **Nepusz T, Csardi G. 2006.** The igraph software package for complex network research.
- 568 **Oksanen J, Simpson G, Blanchet F, Kindt R, Legendre P, Minchin P, O’Hara R, Solymos**
569 **P, Stevens M, Szoecs E, et al. 2022.** vegan: Community Ecology Package.
- 570 **Öpik M, Vanatoa A, Vanatoa E, Moora M, Davison J, Kalwij JM, Reier Ü, Zobel M. 2010.**
571 The online database MaarjAM reveals global and ecosystemic distribution patterns in arbuscular
572 mycorrhizal fungi (Glomeromycota). *New Phytologist* **188**: 223–241.
- 573 **Peaucelle M, Bacour C, Ciais P, Vuichard N, Kuppel S, Peñuelas J, Beilelli Marchesini L,**
574 **Blanken PD, Buchmann N, Chen J, et al. 2019.** Covariations between plant functional traits
575 emerge from constraining parameterization of a terrestrial biosphere model. *Global Ecology and*
576 *Biogeography* **28**: 1351–1365.
- 577 **Petersen T. 2022.** tidygraph: A Tidy API for Graph Manipulation.
- 578 **Peterson ML, Bailes G, Hendricks LB, Pfeifer-Meister L, Reed PB, Bridgham SD, Johnson**
579 **BR, Shriver R, Waddle E, Wroton H, et al. 2020.** Latitudinal gradients in population growth
580 do not reflect demographic responses to climate. *Ecological Applications*.
- 581 **Pickles BJ, Wilhelm R, Asay AK, Hahn AS, Simard SW, Mohn WW. 2017.** Transfer of ¹³C
582 between paired Douglas-fir seedlings reveals plant kinship effects and uptake of exudates by
583 ectomycorrhizas. *New Phytologist* **214**: 400–411.
- 584 **R Core team. 2015.** R Core Team. *R: A Language and Environment for Statistical Computing.*
585 *R Foundation for Statistical Computing, Vienna, Austria. ISBN 3-900051-07-0, URL*
586 *<http://www.R-project.org/>. 55: 275–286.*
- 587 **Reed PB, Bridgham SD, Pfeifer-Meister LE, DeMarche ML, Johnson BR, Roy BA, Bailes**
588 **GT, Nelson AA, Morris WF, Doak DF. 2021a.** Climate warming threatens the persistence of a
589 community of disturbance-adapted native annual plants. *Ecology* **102**: e03464.

590 **Reed PB, Peterson ML, Pfeifer-Meister LE, Morris WF, Doak DF, Roy BA, Johnson BR,**
591 **Bailes GT, Nelson AA, Bridgham SD. 2021b.** Climate manipulations differentially affect plant
592 population dynamics within versus beyond northern range limits (I Stott, Ed.). *Journal of*
593 *Ecology* **109**: 664–675.

594 **Reed PB, Pfeifer-Meister LE, Roy BA, Johnson BR, Bailes GT, Nelson AA, Boulay MC,**
595 **Hamman ST, Bridgham SD, Pfeifer-Meister LE, et al. 2019.** Prairie plant phenology driven
596 more by temperature than moisture in climate manipulations across a latitudinal gradient in the
597 Pacific Northwest, USA. *Ecology and Evolution* **9**: 3637–3650.

598 **Reed PB, Pfeifer-Meister LE, Roy BA, Johnson BR, Bailes GT, Nelson AA, Bridgham SD.**
599 **2021c.** Introduced annuals mediate climate-driven community change in Mediterranean prairies
600 of the Pacific Northwest, USA (S Irl, Ed.). *Diversity and Distributions* **00**: 1–12.

601 **Ruiz-Vera UM, De Souza AP, Long SP, Ort DR. 2017.** The role of sink strength and nitrogen
602 availability in the down-regulation of photosynthetic capacity in field-grown *Nicotiana tabacum*
603 L. at elevated CO₂ concentration. *Frontiers in Plant Science* **8**: 998.

604 **Selosse MA, Richard F, He X, Simard SW. 2006.** Mycorrhizal networks: des liaisons
605 dangereuses? *Trends in Ecology and Evolution* **21**: 621–628.

606 **Silva LCR, Lambers H. 2021.** Soil-plant-atmosphere interactions: structure, function, and
607 predictive scaling for climate change mitigation. *Plant and Soil*: 1–23.

608 **Silva LCR, Salamanca-Jimenez A, Doane TA, Horwath WR. 2015.** Carbon dioxide level and
609 form of soil nitrogen regulate assimilation of atmospheric ammonia in young trees. *Scientific*
610 *reports* **5**: 13141.

611 **Simard SW, Perry DA, Jones MD, Myrold DD, Durall DM, Molina R. 1997.** Net transfer of
612 carbon between ectomycorrhizal tree species in the field. *Nature* **388**: 579–582.

613 **Smith T, Heger A, Sudbery I. 2017.** UMI-tools: modeling sequencing errors in Unique
614 Molecular Identifiers to improve quantification accuracy. *Genome Research* **27**: 491–499.

615 **Smith SE, Read DJ (David J). 2008.** *Mycorrhizal symbiosis*. Academic Press.

616 **Soudzilovskaia NA, Vaessen S, Barcelo M, He J, Rahimlou S, Abarenkov K, Brundrett**
617 **MC, Gomes SIF, Merckx V, Tedersoo L. 2020.** FungalRoot: global online database of plant
618 mycorrhizal associations. *New Phytologist* **227**: 955–966.

- 619 **Spencer MW, Roy BA, Thornton TE, Silva LCR, McGuire KL. 2023.** Logging has legacy
620 effects on the structure of soil fungal communities several decades after cessation in Western
621 Cascade forest stands. *Frontiers in Forests and Global Change* **6**: 41.
- 622 **Sperling O, Silva LCR, Tixier A, Th eroux-Rancourt G, Zwieniecki MA. 2017.** Temperature
623 gradients assist carbohydrate allocation within trees. *Scientific Reports* **7**: 3265.
- 624 **Tedersoo L, Bahram M, Zobel M. 2020.** How mycorrhizal associations drive plant population
625 and community biology. *Science* **367**.
- 626 **Tegeder M, Masclaux-Daubresse C. 2018.** Source and sink mechanisms of nitrogen transport
627 and use. *New Phytologist* **217**: 35–53.
- 628 **Vandegrift R, Roy BA, Pfeifer-Meister L, Johnson BR, Bridgham SD. 2015.** The herbaceous
629 landlord: integrating the effects of symbiont consortia within a single host. *PeerJ* **3**: e1379.
- 630 **Walder F, van der Heijden MGA. 2015.** Regulation of resource exchange in the arbuscular
631 mycorrhizal symbiosis. *Nature Plants* **1**.
- 632 **Ward EB, Duguid MC, Kuebbing SE, Lendemer JC, Bradford MA. 2022.** The functional
633 role of ericoid mycorrhizal plants and fungi on carbon and nitrogen dynamics in forests. *New*
634 *Phytologist*.
- 635 **Weremijewicz J, Sternberg L da SLO, Janos DP. 2016.** Common mycorrhizal networks
636 amplify competition by preferential mineral nutrient allocation to large host plants. *New*
637 *Phytologist* **212**: 461–471.
- 638 **Werner C, Dubbert M. 2016.** Resolving rapid dynamics of soil-plant-atmosphere interactions.
639 *New Phytologist* **210**: 767–769.
- 640 **Wilson H, Johnson BR, Bohannon B, Pfeifer-Meister LE, Mueller R, Bridgham SD. 2016.**
641 Experimental warming decreases arbuscular mycorrhizal fungal colonization in prairie plants
642 along a Mediterranean climate gradient. *PeerJ* **2016**: 1–22.
- 643
- 644 **Supporting information**
- 645 Table S1. List of species at each site with number of leaf samples per species.
- 646 Table S2. Collection dates for each time point at each site.
- 647 Table S3. List of fungal ASVs by annuals and perennials.
- 648 Figure S1. Enrichment decreases over time in labelled plants.
- 649 Figure S2. Receiver enrichment did not correlate with donor enrichment.

- 650 Figure S3: Annuals are more greatly enriched with ^{15}N than perennials.
- 651 Figure S4. No trend in ^{15}N enrichment across site and rain exclusion treatment.
- 652 Figure S5. Limited soil enrichment 21 days after labelling.
- 653 Figure S6. Histogram of connectivity metrics showing left skew.